

REVEALING THE GEOLOGIC AND FLUVIAL HISTORY OF HEBRUS VALLES AND HEPHAESTUS FOSSAE ON MARS. S. Nerozzi¹, B.S. Tober¹, M.R. Ortiz², J.W. Holt¹. ¹Lunar and Planetary Laboratory, University of Arizona, Tucson, AZ (nerozzi@lpl.arizona.edu), ²Jackson School of Geosciences, University of Texas at Austin.

Introduction: Hebrus Valles (HV) and Hephaestus Fossae (HF) are well-preserved examples of Early Amazonian outflow channel systems carved into bedrock in SE Utopia Planitia, Mars (17-25 °N, 118-129 °E, Fig. 1). They exhibit a diverse set of morphologies indicative of formation by one or more liquid water outflow events, possibly initiated by magmatic intrusion, melting and cracking of the cryosphere [1-4]. However, little is known about their history, including both the origin and ultimate fate of the water and resulting sediments. This represents a significant gap in our understanding of geologic processes occurring in the Amazonian Period. Thanks to extensive coverage by recent datasets, it is now feasible to study the evolution of the HV-HF outflow channel systems with an integrated analysis of diverse, complementary data. These include high-resolution visible imagery, multispectral infrared datasets, surface and subsurface radar sounding, and stereo-derived digital terrain models (DTMs).

Methods: The initial task of this study is chronostratigraphic geologic mapping of the HV-HF region (Fig. 1). We integrate the analysis of a context camera (CTX) mosaic basemap with stereo-derived CTX DTMs, Shallow Radar (SHARAD) surface reflectivity, and Thermal Emission Imaging Spectrometer (THEMIS) decorrelation stretches. This task is followed by the detailed reconstruction of the sequence of geological processes and events based on the identification of morphological and thermophysical facies in a subset of the study region. We employ impact crater statistical analysis to determine geologic unit ages (and thus maximum ages of outflow channels), and history of subsurface water exposed in the ejecta of large impacts.

We analyzed over 300 Shallow Radar (SHARAD) 2D profiles over the entire study area, and traced subsurface reflectors. Clutter simulations based on high resolution DTMs allowed us to distinguish returns that appear in the subsurface but originate from off-nadir surface relief [5]. In addition to subsurface mapping, numerous studies have demonstrated the ability of reflectivity analysis to provide quantitative descriptions of scattering properties and dielectric permittivity of the surface and the shallow subsurface in SHARAD data [e.g., 6]. We applied similar techniques to a subset of SHARAD profiles crossing HV to obtain a quantitative description of near-surface reflectivity.

Preliminary studies and results: *Geologic and facies mapping.* Fig. 3 illustrates examples of five sample facies mapped in our preliminary study using CTX images. We identified a total of 23 facies within the HV-

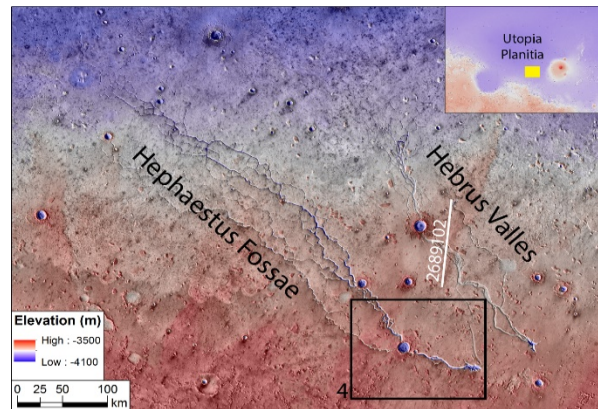


Figure 1: THEMIS IR Day mosaic overview of the study region in the broader context of Utopia Planitia. The black box indicates the location of Fig. 4, the white line indicates the radar profile ground track in Fig. 2.

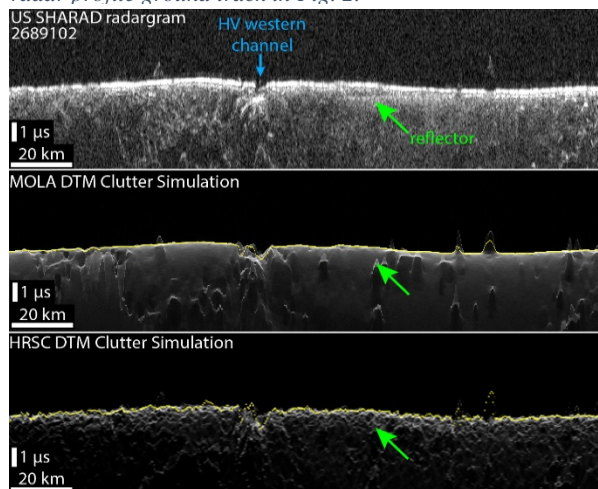


Figure 2: Sample of SHARAD profile showing a subsurface reflector. Clutter simulations below shows that only diffuse scattering is present at that location.

HF study region, which will be used to reconstruct the origin and evolution of the outflow channels in detail. Preliminary impact crater statistical analysis reveals that the HV-HF channels are carved into $2.4^{+0.2}_{-0.2}$ Ga terrains, placing their activity well into the Amazonian Period.

Subsurface radar sounding. Radar subsurface mapping reveals numerous clusters of shallow reflectors, which we divide into three categories based on their location. One large cluster of reflectors is associated with terrains of Hyblaeus Fossae and Granicus Valles. A second cluster, smaller in extent, is located to the SE of HV. The third group comprises reflectors near the outflow channels of HV, with a depth ranging from ~45 m assuming a basaltic subsurface composition ($\epsilon' = 8.8$, [7]) to ~60 m assuming pure water ice ($\epsilon' = 3.1$ [e.g., 8]). These depths are not compatible with the detection of

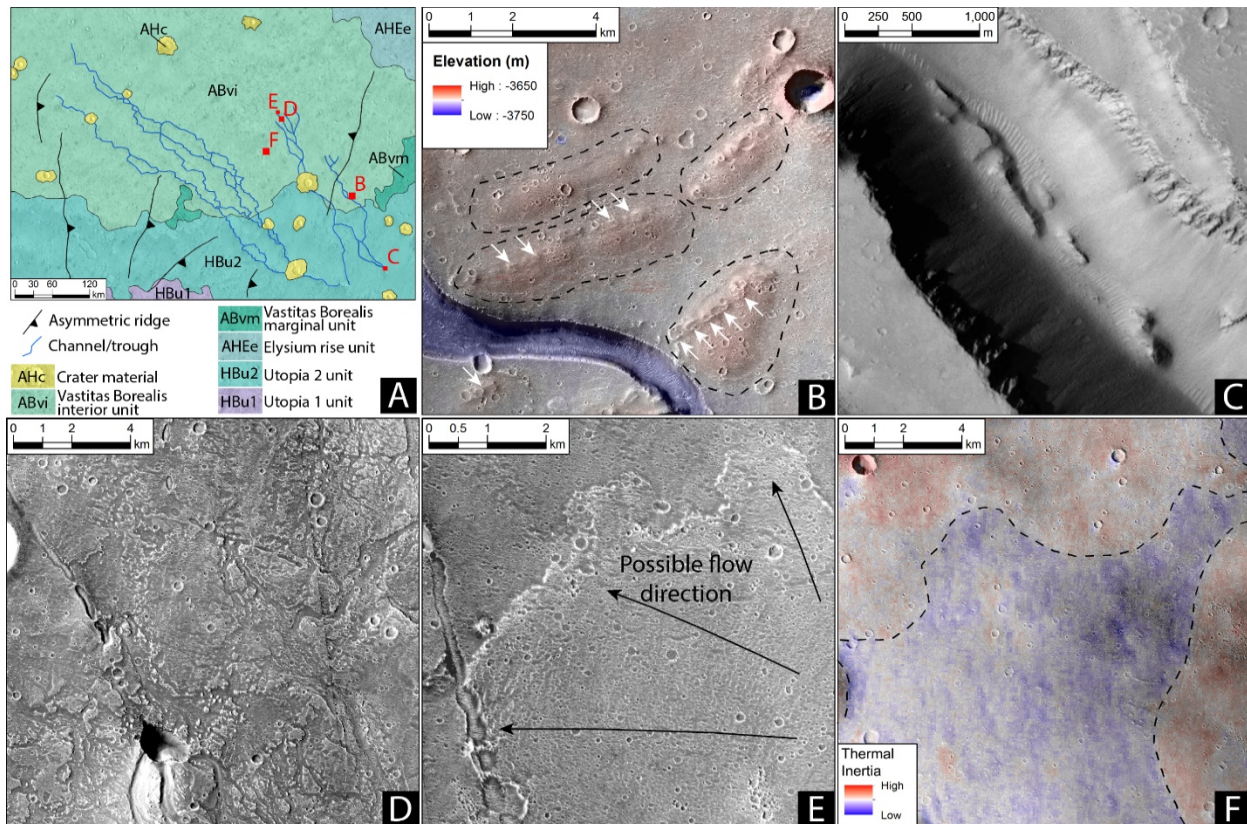


Figure 3: Re-digitized sample of the ref. [3] geologic map in the HV-HF region, with locations of geologic facies in other panels (red). (B) The pitted cone terrain (white arrows) and inflated terrain (black dashed line) often occur together; CTX DTM elevation basemap. (C) Linear ridge (within pit) facies. (D) Distributary channel-incised terrain, which cuts through the lobate and undulated rough terrain shown in panel E. (E) Lobate and undulated rough terrain, which is found only in the terminal region of HV. (F) Example of the low TI smooth terrain, bounded by lobate terrain with higher TI; the basemap is the THEMIS IR night mosaic.

the base of the resistant layer seen in nearby outcrops at <30 m depth. Moreover, reflectors appear to pinch-out or vary in depth considerably, and are all located within the topographic expression of a wrinkle ridge, suggesting a structural, rather than stratigraphic, origin.

Surface radar reflectivity. Quantitative analysis of a subset of 24 profiles crossing knobbed terrains in HV reveals a strong variability in surface reflectivity (Fig. 4). This could be due to a more heterogeneous subsurface at site A that could result from a high-energy sedimentary environment, but a complete analysis including surface roughness is required to fully evaluate the data.

Acknowledgements: This work is supported by NASA MDAP grant NNN18ZDA001N.

References: [1] Christiansen E.H. and Hopler J.A. (1987) *NASA Rep. Planet. Geol. & Geophys. Prog.*, 1986, 307-309. [3] Tanaka K.L. et al. (2005) *USGS, SIM2888*. [4] Rodriguez, J.A. et al. (2012) *GRL*, 39, L22201. [5] Choudhary, P. et al. (2016) *GRSL*, 13, 1285-1289. [6] Grima et al., (2012) *Icarus* 220, 84-99. [7] Nunes D.C. and Phillips R.J. (2006) *JGR*, 111, E06S2. [8] Heggy et al. (2008) *LPSC XXXIX*, Abstract #2471.

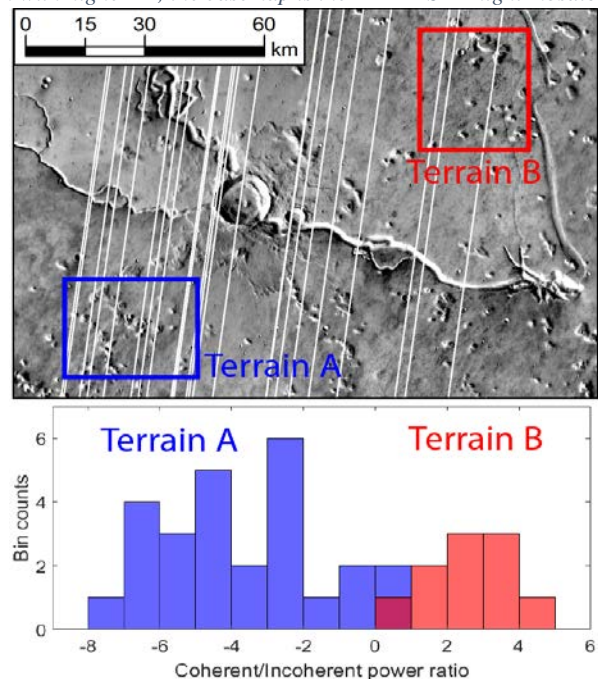


Figure 4: Preliminary test of coherent/incoherent power extraction from 24 SHARAD profiles (white lines).